Reinforcement Learning Impedance Control of a Robotic Prosthesis to Coordinate With Human Intact Knee Motion

Ruofan Wu¹⁰, Minhan Li¹⁰, *Graduate Student Member, IEEE*, Zhikai Yao¹⁰, Wentao Liu¹⁰, Jennie Si¹⁰, *Fellow, IEEE*, and He Huang¹⁰, *Senior Member, IEEE*

Abstract—This study aims to demonstrate reinforcement learning tracking control for automatically configuring the impedance parameters of a robotic knee prosthesis. While our previous studies involving human subjects have focused on tuning the impedance control parameters to meet a fixed, subjectively prescribed target motion profile to enable continuous walking with human-in-theloop, in this paper we develop a new tracking control solution for a robotic knee to mimic the motion of the intact knee. As such, we replaced the prescribed target knee motion by an automatically generated profile based on the intact knee. As the profile of the intact knee varies over time due to human adaptation, we are presented with a challenging tracking control problem in the context of classical control theory. By formulating the "echo control" of the robotic knee as a reinforcement learning problem, we provide a promising new tool for real-time tracking control design without explicitly representing the underlying dynamics using a mathematical model, which can be difficult to obtain for a human-robot system. Additionally, our results may inspire future studies and new robotic prosthesis impedance control designs that can potentially coordinate between the intact and the robotic limbs toward daily use of the robotic device.

Index Terms—Reinforcement learning, prosthetics and exoskeletons, compliance and impedance control, physical human-robot interaction.

I. INTRODUCTION

POWERED lower limb prosthesis promises to help lower limb amputees to restore normative gait by mimicking the function of biological joints [1]. One of the limitations in current prosthesis control is a lack of adaptation to human users who have different physical conditions and show different gait compensation patterns. Often, the control parameters of these

Manuscript received January 8, 2022; accepted May 9, 2022. Date of publication June 1, 2022; date of current version June 13, 2022. This letter was recommended for publication by Associate Editor L. De Michieli and Editor P. Valdastri upon evaluation of the reviewers' comments. The work of Jennie Si was supported by National Science Foundation under Grants 1563921 and 1808752, and the work of He Huang was supported by National Science Foundation under Grants 1563454 and 1808898. (Corresponding authors: Jennie Si; He Huang.)

Ruofan Wu, Zhikai Yao, and Jennie Si are with the School of Electrical, Computer and Energy Engineering, Arizona State University, Tempe, AZ 85287 USA (e-mail: ruofanwu@asu.edu; zacyao.cn@gmail.com; si@asu.edu).

Minhan Li, Wentao Liu, and He Huang are with the UNC/NCSU Department of Biomedical Engineering, NC State University, Raleigh, NC 27695 USA, and also with the University of North Carolina at Chapel Hill, Chapel Hill, NC 27599 USA (e-mail: mli37@ncsu.edu; wliu29@ncsu.edu; hhuang11@ncsu.edu).

Digital Object Identifier 10.1109/LRA.2022.3179420

devices, such as joint impedance parameter values within a finite state impedance setting, must be manually tuned to provide personalized gait assistance [2]–[4]. This is a challenging control task. First of all, one has to decide what the robot control objective is as it is difficult to describe mathematically a control design objective due to a lack of understanding of human-prosthesis system [5]–[7]. In addition, it is very difficult to model the interacting dynamics of human-prosthesis systems, an issue further complicated by large variations between and within humans. Another challenge stems from a physical constraint that taking measurements of human performance such as metabolic cost takes long evaluation time [8], and these measurements are affected by confounding factors such as limb loading and socket fit, and thus unpractical to be used for controlling a robotic prosthesis for long-term and daily use.

To address these challenges yet still making the problem tractable, we first tested the feasibility of automatically tuning of 12 impedance parameters of a prosthesis knee by using model-free reinforcement learning (RL) to meet a prescribed prosthesis knee movement profile in gait, which is time invariant [7], [9], [10]. These algorithms successfully learned the tuning policy and completed the tuning procedure while a human walked with the prosthesis. Yet, a serious limitation is that prescribing knee movement profiles for each person and for each task is not realistic or even possible. And also, as humans adapt to walking with a prosthesis, a fixed robotic knee profile potentially hinder the coordination between the human and the robot.

Now the question is how to formulate realistic and feasible target movement profiles for robotic limb control. An interesting approach determined prosthesis joint gait pattern is mirroring the contralateral joint motion in the intact limb as bilateral lower limb coordination is essential for human locomotion. Grimes *et al.* developed a mirror control scheme for the stance phase only [11]. In order to control a complete gait cycle, the echo controller tracked the sound limb's knee angle trajectory while a prescribed trajectory was applied for the swing phase only. Bernal-Torres *et al.* applied a Kalman filter based approach to realize echo control [12]. However, the prosthesis prototype was suspended from above the test bench without touching the ground. The result of this approach was not demonstrated on human subjects for continuous walking. As shown, these approaches focused on a segment of a complete gait cycle.

2377-3766 © 2022 IEEE. Personal use is permitted, but republication/redistribution requires IEEE permission. See https://www.ieee.org/publications/rights/index.html for more information.

Another potential idea is to make use of a known coordination mechanism from unamputated joint motions, which in turn, to guide the prosthetic joint movement pattern. Several previous studies examined this concept centering on ipsilateral hip-knee-ankle coordination defined in gait biomechanics to control prosthesis knee and ankle by monitoring residual hip motion [13]. Note that, all the above studies utilized position control at low level joint operation. This may be of safety concerns. Instead, the finite state impedance control strategy is a more feasible approach in comparison, and is usually adopted to meet compliance requirements for user safety [14].

Inspired by both previous research on multi-joint coordination for prosthesis control and our own success in using model-free RL for high-dimensional impedance control parameter tuning, we aimed to control a robotic knee by mirroring the intact knee motion. Thus the contributions of this study include the following. For the first time, we achieved real-time human testing of RL tracking control for tuning impedance parameters of a robotic knee to mirror a time varying movement profile of an intact knee during human-prosthesis co-adaptation. We provided a successful implementation procedure for a RL tracking controller to advance from simulation [15] to realistic continuous walking. We demonstrated real-time RL tracking control as a viable solution approach beyond classical tracking control designs. Lastly, we contributed initial yet important knowledge on human adaption to powered prosthesis, a phenomena that could potentially facilitate understanding of physical humanprosthesis interaction.

The rest of the paper is organized as follows. Section II introduces detailed methods to facilitate this study. Section III describes experimental set up to carry out the study. Section IV includes systematic processing and testing results, while the final section concludes our major findings and discusses implications of the results.

II. METHODS

The finite state machine (FSM) impedance controller (IC), or FSM-IC, is the most adopted framework for intrinsic control of prosthetic devices. We also rely on FSM-IC with its impedance parameter settings automatically tuned by a reinforcement learning tracking controller to enable stable, continuous walking. We carry out the investigations using human subject testing.

A. Finite State Machine Impedance Control

Fig. 1 depicts the RL based solution approach of automatic tracking control for a robotic knee to mirror the intact knee joint motion. Refer to Fig. 2(a), a gait cycle is divided into four phases in the FSM-IC: stance flexion (STF), stance extension (STE), swing flexion (SWF) and swing extension (SWE). The phase transitions are determined by knee motion and gait events (heel strike and toe-off) that are obtained from vertical ground reaction forces of both legs. In each phase of the FSM, three impedance parameters (stiffness K, damping B, and equilibrium position θ_e) are provided as inputs to the FSM-IC for impedance

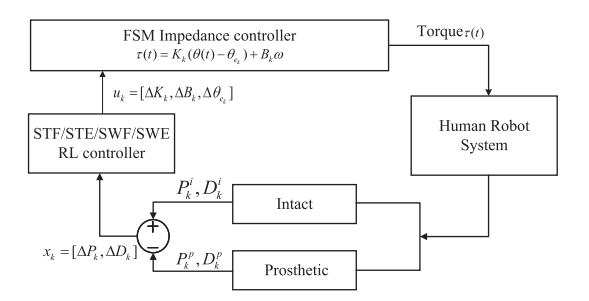


Fig. 1. Schematic of RL-based tracking control of a robotic knee.

parameter update cycle k:

$$I_k = [K_k, B_k, \theta_{e_k}]. \tag{1}$$

The knee joint torque is consequently generated by the following first principle equation

$$T_k = K_k(\theta - \theta_{e_k}) + B_k\omega. \tag{2}$$

The RL tracking controller will adjust these parameters, i.e.,

$$u_k = [\Delta K_k, \Delta B_k, \Delta \theta_{e_k}] \tag{3}$$

so that the updated impedance parameters, $I_{k+1} = I_k + u_k$, are applied to the FSM-IC to generate knee torque and thus enable walking.

B. Reinforcement Learning Tracking Control

Even though we have successfully demonstrated regulation control of a robotic prosthesis to meet a fixed motion profile [7], [9], [10], tracking a moving target profile has not been demonstrated especially when we need to tune a large number of impedance parameters to achieve safe human machine interaction. To formulate a reinforcment learning control problem, we need to clearly define the states, control, and cost objective function to be optimized by tuning control variables which in this case are the impedance parameters (a total of 12, 3 for each of the 4 phases). Refer to Fig. 2(a) by which we will define the state variables of the RL controller. For an impedance parameter update cycle index k, the intact knee motion featured by the peak knee angle P_k^i (degrees) and duration D_k^i (seconds) are measured. Similarly, we measure the peak knee angle P_k^p and duration D_k^p of the prosthesis. Let ΔP_k and ΔD_k (Fig. 2(a)) denote the peak value error and duration time error, respectively, i.e.,

$$\Delta P_k = P_k^p - P_k^i,$$

$$\Delta D_k = D_k^p - D_k^i.$$
(4)

We have thus formulated the state x_k as

$$x_k = [\Delta P_k, \Delta D_k]. \tag{5}$$

We denote a RL state feedback tracking control policy as

$$u_k = h(x_k). (6)$$

Then we consider the instantaneous cost in a quadratic form

$$U(x_k, u_k) = x_k^T R_x x_k + u_k^T R_u u_k,$$
 (7)

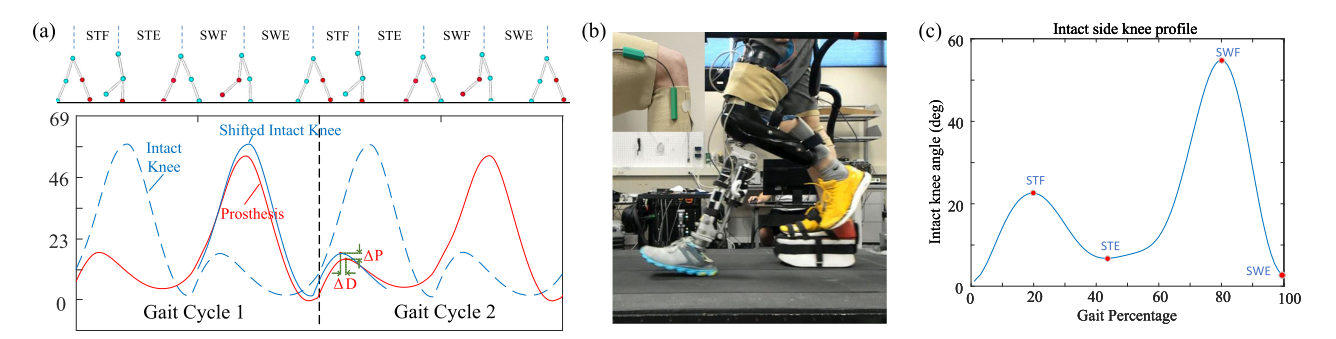


Fig. 2. (a) Two complete gait cycles with each divided into 4 phases. To realize echo control, the peak error and duration time error were obtained based on the intact knee profile and the half-cycle delayed prosthetic knee profile. Red: Prosthetic knee angle profile. Dashed Blue: Intact knee angle profile. Solid blue: intact knee angle shifted half cycle to provide a tracking reference for the prosthetic knee. (b) Human testing environment. (c) Feature extraction from the intact knee. It was based on the trajectory of the intact knee profile. Two peaks and troughs were used to determine the feature angles and phase transitions.

where $R_x \in \mathbb{R}^{2 \times 2}$ and $R_u \in \mathbb{R}^{3 \times 3}$ are positive definite matrices. An infinite horizon discounted cost was used as tracking control objective. This allows the tracking controller to minimize the error between intact knee profile features and the measured prosthesis profile features. Refer to Fig. 1, four respective PICE controllers were trained for each of the four phases of a gait. The four controllers were of the same structure and used the same procedure to train. We applied our previously developed policy iteration with constraint embedded (PICE) [9] reinforcement learning algorithm for tracking.

The following steps iterated until tuning termination condition described in Section IV was met. First, the peak knee angle and duration $[P_k,D_k]$ were measured after every gait cycle using the feature selection rule described in Section IV. Second, the tracking error $x_k = [\Delta P_k, \Delta D_k]$ was obtained using (6) which served as states of the RL control implemented by PICE. Third, the PICE controller was updated based on (14) in [9] to solve a quadratic programming (QP) problem. The impedance parameter increments $\Delta I = [\Delta K, \Delta B, \Delta \theta_e]$ were thus obtain as the output of PICE.

The updated impedance parameters were then used as shown in Fig. 1 to enable the next gait cycle(s). Specifically, the knee torque was computed based on (2) given the impedance parameters, which would be used in the intrinsic controller to compute $\tau(t)$. The control torque $\tau(t)$ results in the kinematic gait profiles as shown in Fig. 2(a). In turn, state variables are exacted according to (5) for gait cycle k. These steps were repeated until meeting termination condition.

III. EXPERIMENT SETUP

The experimental protocol was approved by the Institutional Review Board at the University of North Carolina at Chapel Hill. During the experiment, subjects wore a powered knee prosthesis and walked on a treadmill at a constant speed of their preferences as shown in Fig. 2(b).

A. Human Data Collection

Human experiment setup is as shown in Fig. 2. Prior to an experiment, a subject was equipped with a fall-arrest harness for safety assurance. An 'L' shaped socket was used to allow

an able-bodied subject to fit into the prosthetic knee and walk with the powered prosthesis. Subjects were trained to walk with the powered prosthesis for approximately 5 hours to become accustomed to and feel confident to walk on a treadmill wearing a prosthesis. Each experiment session lasted about 2 hours. After 10 or so impedance updates taking about 20 minutes of experimentation, subjects took a 5–10 minute break. Or subjects took breaks as needed.

The robotic knee prosthesis used in this experiment was designed based on [4]. This prosthesis used a slider-crank mechanism, where the knee motion was driven by the rotation of the moment arm powered by the DC motor through the ball screw. An embedded potentiometer was used to record the robotic knee kinematics and an embedded load cell was used to trigger the phase transition. The ground reaction force was also recorded through the instrumented treadmill (1000 Hz; Bertec Corp., Columbus, OH, USA) during the experiments to help determine the intact limb phase transition. The prosthesis was controlled by a LabVIEW and MATLAB integrated system in a desktop PC with a 100 Hz sampling rate of kinematic signals [4]. To acquire the intact knee kinematics, a goniometer provided by Biometrics Ltd. was used to measure the knee angle (Fig. 2(b)).

B. Human Data Pre-Processing

In this study, we recorded experimental data of two ablebodied human subjects and a transfemoral amputee subject. Kinematics of both knee profiles were collected to derive knee angle and phase duration for each of the four phases for each subject so that state variables as in (5) were obtained. The recorded ground reaction force measurements were segmented using an alignment with the start of each tuning iteration. Note that the impedance parameters were updated every 4 gait cycles, during which the prosthetic knee was controlled by the same set of impedance parameters. Specifically, the ground reaction force measurements and the knee kinematics were filtered by a low-pass filter with a cutoff frequency of 20 Hz. Then we identified the gait events of heel strike and toe off using vertical ground reaction force with a threshold value of 30 N to determine gait transitions. A Dempster-Shafer based state transition rule

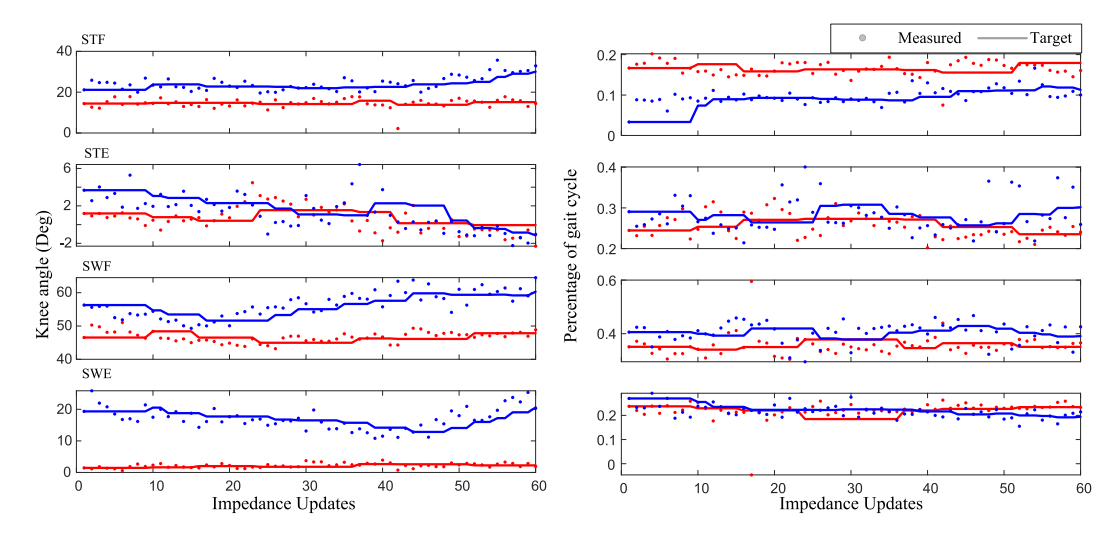


Fig. 3. Target feature extraction from intact knees of AB1 (blue) and AB2 (red), respectively. The Peak angle (Left) and duration (Right) for 4 phases were calculated as described in Section IV A.

was applied [4]. The phase transitions were then determined by combining decision factors including the ground reaction force, the knee angle and angular velocity.

C. Intact Knee Feature Extraction

Extracting intact knee profile features is a new challenge for tracking control in this study. The intact knee features to be tracked by the robotic knee are denoted as $[P_k^i, D_k^i]$ in (4) which were obtained from recorded kinematic data described above. In human experiments, unlike the robotic knee with embedded sensors to reliably measure knee kinematics and thus to parse phase transitions in FSM, the intact limb kinematics can only be determined from measured knee angle waveforms and ground reaction force measurements.

Specifically, first, the knee profile was segmented into gait cycles according to heel strike events. Let $[\tilde{P}_k^i, \tilde{D}_k^i]$ denote peak/trough feature points as shown in Fig. 2(c). They correspond to the four characteristic points of a gait cycle where, for the swing phase, the maximum point was the feature point for SWF and the minimum point between maximum point and next gait is the feature point for SWE. For the stance phases, the peak and the trough between gait start and maximum point were the feature points for STF and STE, respectively.

The next challenge is to overcome human variances. Tracking the intact knee motion can only take place with a delay of one gait cycle. Also as expected, significant human variance and measurement noise can corrupt intact knee measurements to be tracked by the robotic knee. To capture the key timing varying features of the intact knee during human adaptation, we placed a bound between two consecutive features of the intact knee and used a running average to generate the target profile for the robotic knee to track. Specifically, for an impedance parameter update cycle k, the peak angle and duration from the intact limb \tilde{P}^i_k and \tilde{D}^i_k was averaged every L (L=10 in this study because the convergence criteria required the error within the tolerance bounds for 8 out of 10 steps) consecutive measurements to obtain

 \bar{P}_k^i and \bar{D}_k^i . For initialization, features of the first gait was used.

$$\bar{P}_{k}^{i} = \frac{\sum_{m=0}^{L-1} \tilde{P}_{k-m}^{i}}{L},$$

$$\bar{D}_{k}^{i} = \frac{\sum_{m=0}^{L-1} \tilde{D}_{k-m}^{i}}{L}.$$
(8)

Then as summarized in (9) below, \bar{P}_k^i was compared to the previous target features P_{k-1}^i . If the two does not differ greatly (i.e., within a threshold $\epsilon=1.5$ degree which must be smaller than tolerance bound) compared to the tracking error tolerance, then \bar{P}_k^i and \bar{D}_k^i remained at their respective previous target values. Otherwise, new intact knee features were to be used for tracking.

$$[P_k^i, D_k^i] = \begin{cases} [P_{k-1}^i, D_{k-1}^i] & \text{if } |P_{k-1}^i - \bar{P}_k^i| \le \epsilon, \\ [\bar{P}_k^i, \bar{D}_k^i] & \text{if } |P_{k-1}^i - \bar{P}_k^i| > \epsilon \end{cases}$$
(9)

Fig. 3 demonstrates intact knee target features over time (impedance update index) as a result of processing by (8) and (9). Specifically, the solid lines are features directly from measurements

IV. RESULTS

Two able-bodied (AB) and one transfemoral amputee (TF) subjects participated in the human experiments. Two AB subjects walked with the robotic knee prosthesis via an L-shaped adapter. The three subjects walked at different speeds of their own preference, 0.65 m/s for AB1, 0.7 m/s for AB2 and 0.8 m/s for TF, respectively. The tracking error tolerance was 2 degrees for peak error and 3% for duration error for 8 out of 10 consecutive impedance updates. A safety bound was placed on the robotic knee to physically prevent it from causing harm to test subjects. It was 1.5 times the standard deviations of the knee kinematic peak values observed in each of the four phases [16] corresponding to [10.5,7.5,9,6] degrees for peak angle errors and [12%, 12%, 12%, 12%] for duration errors.

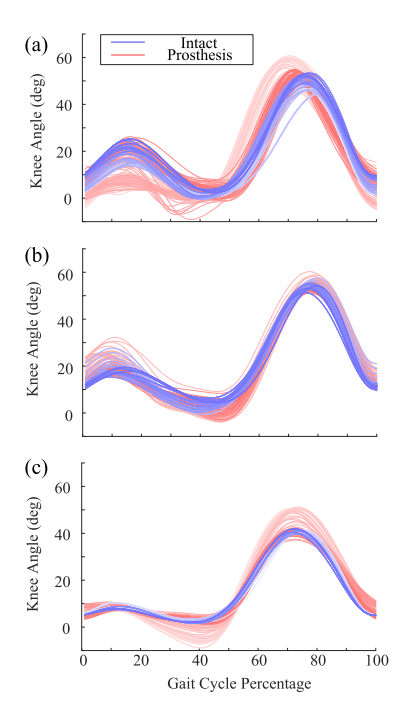


Fig. 4. Test results: A: AB1, B: AB2. C:TF. Knee profiles of the intact limbs and prosthetic limbs for both test subjects update by update. Colors from light to dark indicate time progression of control tuning.

Fig. 4 represents adaptation of both the intact and the robotic knee profiles of all subjects. The initial knee profiles of the intact and the robotic knee profiles (light blue and light red, respectively) were quite far from one other as the initial robotic knee impedance parameters were randomly generated. As learning proceeded, the robotic knee profile approached that of the intact knee. Both the intact and the prosthetic knee profiles eventually met at the time when the robotic knee tracking control terminated updates as error tolerance criteria were met.

Fig. 5 are peak angle and duration errors for all subjects. Converging behavior associated with both peak angle and duration is shown for all four phases and for all subjects where convergence is defined for the errors to stay within tolerance bounds for 8 out of 10 consecutive impedance updates. When inspecting the peak errors and duration errors as defined in Equ. (6), for AB1, peak errors reduced from -4.6 to -1.7 degrees for STF and from 3.6to -0.7 degree for STE. In the swing phases, peak errors reduced from 13.8 to -0.9 degrees for SWF and from -4.7 to -0.8degrees for SWE. For AB2, peak errors of STF and STE reduced from 10 to 0 and from 3 to -0.2 degrees, respectively, while the other two phases initially were within tolerance and remained in the range. For the duration errors, AB1 was consistent during testing so that all four phases remained within tracking error tolerance range. For AB2, an apparent decrease during STE and SWF was observed from 6% to 1.8% and from -6% to -2.5%, respectively, while the other 2 phases maintained a small phase duration error.

Testing results on the amputee subject reveal consistent outcomes as those in tests involving AB subjects. Fig. 5 shows convergence in tracking error to within the tolerance bounds for both peak angle error, from $\left[-3.1, -5.6, 8.76, 2.4\right]$

degrees to [-0.8, 0.1, -0.5, -0.9] degrees, and duration error which remained within tolerance bounds most of the time.

Convergence of learning the control policy is shown in Fig. 6 which reveals how the impedance parameters evolved during tuning for the TF subject testing. Converging behavior of the impedance parameters was observed as they met convergence criteria in last ten updates.

T-test was performed to verify the significance of the results. The three test samples were prepared as follows. For a complete trial of several impedance parameter updates, one test sample contains the first 10 peak errors or duration errors during the first 10 impedance tuning updates, and the other sample contains the last 10 errors during the last 10 impedance updates from convergence. The peak errors of AB1 and TF decreased significantly (p < 0.01) while the duration time errors were not significant (p > 0.01) as it remained within the tracking error tolerance bound during experimental testing. For AB2, both peak errors and duration time errors decreased significantly (p < 0.01).

V. CONCLUSIONS AND DISCUSSION

The three subjects showed different adaptation patterns (Fig. 4): AB1 tends to increase flexion in the STF phase but AB2 and TF tends to reduce flexion. This may suggest that individuals use different approaches to collaborating with the robotic device. This in turns shows that learning based control designs are necessary.

The amputee subject reflected on the test experience of using the echo control strategy in the robotic knee. The subject felt stable during the entire testing procedure and that the echo control was more comfortable than using a prescribed knee profile as target in previous studies the subject had experienced. The subject preferred less flexion during the stance phase which was also shown in the result Fig. 4 under echo control. This has given him more confidence walking with the robotic knee. Interestingly, we observed that the peak angle of STF of the intact side decreased during testing which resulted in less flexion of the prosthetic leg. This may be due to co-adaptation that helped the subject find a more comfortable way to walk. Yet more tests are required to investigate this hypothesis. The echo control developed in this study will enable futures studies of this issue.

In our study, a device such as a goniometer was required to record the intact knee angle. Such a use may not be the best option for practical use. As the first end-to-end study of echo control tested on human subjects for continuous walking in a laboratory, we adopted this approach to demonstrate the concept. Note, however, our control strategy framework and the control algorithm proposed in this work can be directly applied to any approach of specifying a target knee profile. For instance, consider virtual constraints [17], [18] which were used for robot control to coordinate with its human user. Biomimetic virtual constraints describe the joints' geometric relationships and coordinate the kinematics among lower limb joints to drive prosthesis motion. It can be a potential alternative to specifying movement profile for the prosthesis to follow. Furthermore, the rapid development of wearable device makes it possible to

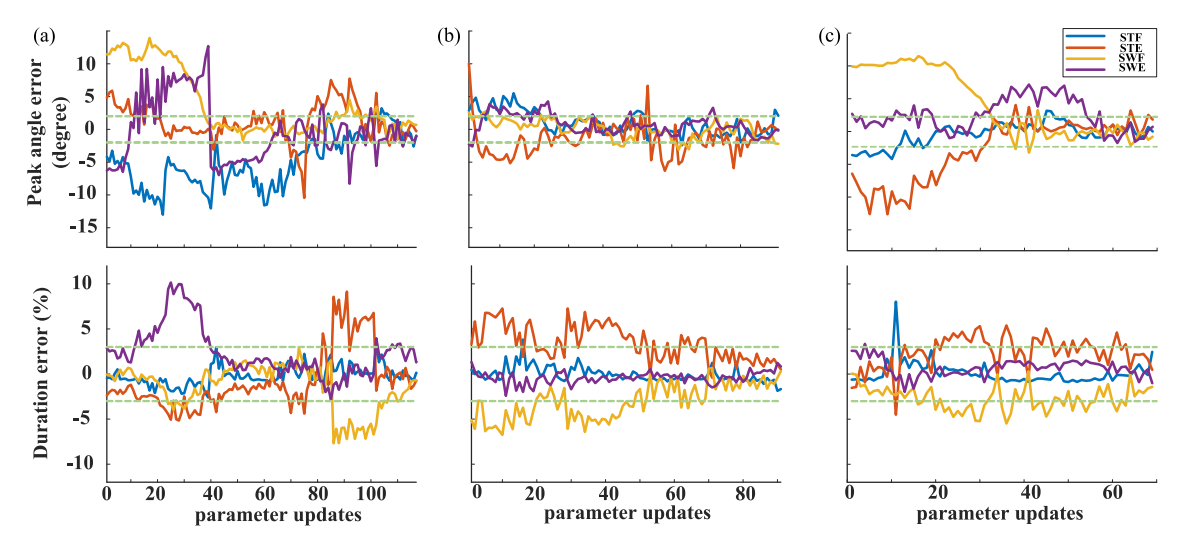


Fig. 5. Tracking errors of all subjects: A: AB1, B: AB2. C:TF. The peak angle errors (top) and duration errors (bottom) during impedance control parameter tuning. Green dashed line indicates the tolerance bounds. The x-axis is the total tuning steps performed to reach the convergence criteria.

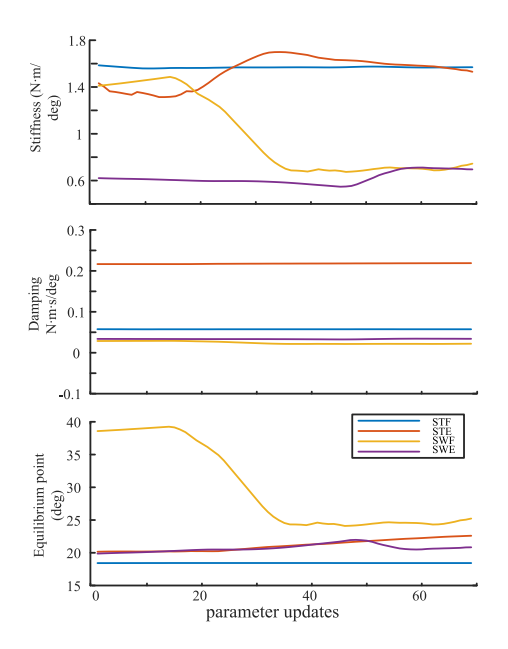


Fig. 6. Evolution of the impedance parameters: stiffness (left), dumping (middle), and equilibrium point (right).

measure joint motion accurately and reliably on a daily basis in the near future [19], [20]. In essence, any approach that properly represents the human intact side kinematics can be implemented using the echo control framework developed in this study.

A reinforcement learning solution framework is a more appropriate approach than supervised learning to addressing the automatic control problem of a robotic knee. Imagine to use supervised learning, collecting training data pairs is a prohibitive task. To fully explore the resulting states, an impractically large set of impedance parameter settings need to be tested, based on which we need to observe the respective states from a human subject. This is not only physically exhausting for human subjects, and it may also cause safety concerns as we do not know how to set the impedance parameters to keep all states and

controls within safety bounds. Implementing a reinforcement learning control usually requires a good exploration.

To provide such exploration, we randomly initialized critic network weights. The actor network weights were either randomly initialized to achieve a broad range of exploration or using a pre-trained policy network with further exploitation in nearby regions. We also applied a small learning rate (less than 0.01) in both networks to encourage exploration as they consequently resulted in extensive updates of parameters. As reported by the TF subject, the learned policy from a randomly initialized one enabled comfortable, stable, and easy to adapt walking for the subject. This may be viewed as a validation of exploration of the policy space.

In this study, the prosthesis was implemented by impedance controller which is a well-established control design framework as a safe and reliable control strategy for lower limb prosthesis [21], [22]. Almost all the commercially available computer-controlled prostheses incorporate impedance control. However, to address daily challenges such as changing from task to task continuously (for example, from level ground walking to stair climbing), in addition to real time control within the finite state impedance control framework, we will also need to include a task planning module, which is not the focus of the current study. Researchers, including those in our own group, have developed different user intent recognition methods. As a future study, these two modules can be integrated and tested toward continuous walking for daily use.

Designing this tracking control system was a major undertaking as it is the first time that human behavior was directly included in our robotic knee control design objective. With the success of this initial study, we will be able to further investigate human adaption when fitted with a prosthetic leg. Although we chose bilateral coordination as the mechanism to determine knee profiles in this study, our approach is also valid for other coordination mechanisms such as ipsilateral joint coordination or full-body coordination. This provides an opportunity to further investigate important human-robot walking

performance measured by, for example, walking symmetry and balance stability as a powered prosthesis can be controlled to directly track intact knee profiles either by spatial measures or by temporal measurements.

Symmetrical walking is not our explicit design objective in this study as our goal is to demonstrate echo control mechanism in robotic knee control. However, reducing gait asymmetry has often been used as the rehabilitation goal in amputee gait training. For this study by mimicking the intact knee, we expect that symmetry is affected. Interestingly, after amputee test, we did a quick inspection on temporal symmetry and found out that the symmetry index decreased from 20% to 10% (improved). This implies that echo control may result in improved symmetry. Yet, further systematic study is needed to test this hypothesis.

REFERENCES

- M. Windrich, M. Grimmer, O. Christ, S. Rinderknecht, and P. Beckerle, "Active lower limb prosthetics: A systematic review of design issues and solutions," *Biomed. Eng. Online*, vol. 15, no. 3, pp. 5–19, 2016.
- [2] H. A. Varol, F. Sup, and M. Goldfarb, "Multiclass real-time intent recognition of a powered lower limb prosthesis," *IEEE Trans. Biomed. Eng.*, vol. 57, no. 3, pp. 542–551, Mar. 2010.
- [3] S. K. Au, H. Herr, J. Weber, and E. C. Martinez-Villalpando, "Powered ankle-foot prosthesis for the improvement of amputee ambulation," in *Proc. 29th Annu. Int. Conf. IEEE Eng. Med. Biol. Soc.*, 2007, pp. 3020–3026.
- [4] M. Liu, F. Zhang, P. Datseris, and H. H. Huang, "Improving finite state impedance control of active-transfemoral prosthesis using dempster-shafer based state transition rules," *J. Intell. Robotic Syst.*, vol. 76, no. 3/4, pp. 461–474, 2014.
- [5] R. E. Quesada, J. M. Caputo, and S. H. Collins, "Increasing ankle push-off work with a powered prosthesis does not necessarily reduce metabolic rate for transtibial amputees," *J. Biomech.*, vol. 49, no. 14, pp. 3452–3459, 2016.
- [6] P. Malcolm, R. E. Quesada, J. M. Caputo, and S. H. Collins, "The influence of push-off timing in a robotic ankle-foot prosthesis on the energetics and mechanics of walking," *J. Neuroengineering Rehabil.*, vol. 12, no. 1, pp. 1–15, 2015.
- [7] Y. Wen, M. Li, J. Si, and H. H. Huang, "Wearer-prosthesis interaction for symmetrical gait: A study enabled by reinforcement learning prosthesis control," *IEEE Trans. Neural Syst. Rehabil.*, vol. 28, no. 4, pp. 904–913, Apr. 2020.
- [8] M. A. Price, P. Beckerle, and F. C. Sup, "Design optimization in lower limb prostheses: A review," *IEEE Trans. Neural Syst. Rehabil. Eng.*, vol. 27, no. 8, pp. 1574–1588, Aug. 2019.

- [9] M. Li, Y. Wen, X. Gao, J. Si, and H. Huang, "Toward expedited impedance tuning of a robotic prosthesis for personalized gait assistance by reinforcement learning control," *IEEE Trans. Robot.*, vol. 38, no. 1, pp. 407–420, Feb. 2022.
- [10] X. Gao, J. Si, Y. Wen, M. Li, and H. Huang, "Reinforcement learning control of robotic knee with human-in-the-loop by flexible policy iteration," *IEEE Trans. Neural Netw. Learn. Syst.*, to be published, doi: 10.1109/TNNLS.2021.3071727.
- [11] D. Grimes and W. Flowers, "Multi-mode above-knee prosthesis controller," in *Control Aspects of Prosthetics and Orthotics*. Amsterdam, The Netherlands: Elsevier, 1983, pp. 43–53.
- [12] M. G. Bernal-Torres, H. I. Medellín-Castillo, and J. C. Arellano-González, "Design and control of a new biomimetic transfemoral knee prosthesis using an echo-control scheme," *J. Healthcare Eng.*, vol. 2018, 2018, Art. no. 8783642.
- [13] D. Quintero, D. J. Villarreal, D. J. Lambert, S. Kapp, and R. D. Gregg, "Continuous-phase control of a powered knee–ankle prosthesis: Amputee experiments across speeds and inclines," *IEEE Trans. Robot.*, vol. 34, no. 3, pp. 686–701, Jun. 2018.
- [14] M. R. Tucker *et al.*, "Control strategies for active lower extremity prosthetics and orthotics: A review," *J. Neuroengineering Rehabil.*, vol. 12, no. 1, pp. 1–30, 2015.
- [15] R. Wu, Z. Yao, J. Si, and H. H. Huang, "Robotic knee tracking control to mimic the intact human knee profile based on actor-critic reinforcement learning," *IEEE/CAA J. Automatica Sinica*, vol. 9, no. 1, pp. 19–30, Jan. 2022.
- [16] M. P. Kadaba, H. Ramakrishnan, and M. Wootten, "Measurement of lower extremity kinematics during level walking," *J. Orthopaedic Res.*, vol. 8, no. 3, pp. 383–392, 1990.
- [17] R. D. Gregg and J. W. Sensinger, "Towards biomimetic virtual constraint control of a powered prosthetic leg," *IEEE Trans. Control Syst. Technol.*, vol. 22, no. 1, pp. 246–254, Jan. 2014.
- [18] S. Kumar, A. Mohammadi, N. Gans, and R. D. Gregg, "Automatic tuning of virtual constraint-based control algorithms for powered kneeankle prostheses," in *Proc. IEEE Conf. Control Technol. Appl.*, 2017, pp. 812–818.
- [19] C. P. Walmsley, S. A. Williams, T. Grisbrook, C. Elliott, C. Imms, and A. Campbell, "Measurement of upper limb range of motion using wearable sensors: A systematic review," *Sports Med.-Open*, vol. 4, no. 1, pp. 1–22, 2018
- [20] I. Poitras et al., "Validity and reliability of wearable sensors for joint angle estimation: A systematic review," Sensors, vol. 19, no. 7, 2019, Art. no. 1555.
- [21] N. Hogan, "Impedance control: An approach to manipulation: Part II— Implementation," J. Dyn. Syst. Meas. Control, vol. 107, no. 1, pp. 8–16, Mar. 1985.
- [22] F. Sup, A. Bohara, and M. Goldfarb, "Design and control of a powered transfemoral prosthesis," *Int. J. Robot. Res.*, vol. 27, no. 2, pp. 263–273, 2008.